Journal of Bionic Engineering (2023) 20:1712–1722
https://doi.org/10.1007/s42235-023-00345-x

RESEARCH ARTICLE

Nanocomposite Electrospun Scaffold Based on Polyurethane/Polycaprolactone Incorporating Gold Nanoparticles and Soybean Oil for Tissue Engineering Applications

Nahideh Asadi[1] · Azizeh Rahmani Del Bakhshayesh[2] · Hadi Sadeghzadeh[2] · Amir Nezami Asl[3] · Sharif Kaamyabi[4] · Abolfazl Akbarzadeh[1,3]

Received: 27 April 2022 / Revised: 24 December 2022 / Accepted: 4 January 2023 / Published online: 8 February 2023

Abstract
Electrospun nanofibers combined with a wide range of functional additives can be used for a various tissue engineering applications due to their desired biomimetic and physicochemical properties. Therefore, the present study was conducted to obtain a highly efficient nanocomposite electrospun scaffold with appropriate physicochemical performance and biological properties based on Polycaprolactone/Polyurethane (PCL/PU) mixed with gold nanoparticles (GNPs) and soybean oil (SO). In the present study, the desired nanofibers were fabricated by electrospinning PCL/PU mixed solution with GNPs and SO. The nanocomposite electrospun PU/PCL/SO/GNP nanofibers were characterized in terms of chemical composition by attenuated total reflectance–Fourier transform infrared spectroscopy (ATR-FTIR), morphological structure by field-emission scanning electron microscopy (FE-SEM), and mechanical and biological properties. The surface topography and wettability were determined by atomic force microscopy (AFM) and water contact angle measurements, respectively. It was found that the presence of GNPs along with SO in the structure of PCL/PU nanofiber created a smoother surface in terms of surface roughness and also a more homogeneous fibrous structure. In addition, it was observed that both SO and GNPs caused an increase in the electrical conductivity of the fibrous mats. In the biocompatibility evaluations by measuring cell viability and cell adherence to the scaffold's surfaces, it was found that adding of SO and GNPs supports fibroblasts. Taken together, the fabricated nanocomposite fibrous scaffolds can be a potential candidate for various tissue engineering purposes.

Keywords Polycaprolactone · Polyurethane · Gold nanoparticles · Soy oil · Bionic

1 Introduction

Regeneration of injured tissues by tissue engineering approaches via developing novel biomaterials has gotten great attention [1]. Tissue engineering provides the structural and functional matrix by the combination of scaffolds, bioactive molecules, and cells to develop responsive constructs for damaged tissues [2]. Scaffold design and components are important factors that can influence tissue engineering outcomes [3]. Various methods, such as electrospinning, gas foaming, 3D printing, and freeze-drying, have been reported to fabricate scaffolds [1, 2, 4]. Nowadays, polymeric electrospun scaffolds have attracted a great deal of attention for tissue engineering applications especially, skin regeneration. Electrospun nanofibers find good advantages such as large surface-to-volume ratio, highly porous extracellular matrix (ECM) resembling membrane, mimicking the fibrous structure of collagen, laminin, and elastin, supporting cell attachment, infiltration, and proliferation for developing tissue engineering scaffolds [5–9]. Recently, new approaches such as multicores-sheath nanostructures have also been developed by coaxial electrospinning technique to produce smart thermo-regulated textiles [10]. PUs, as

✉ Abolfazl Akbarzadeh
akbarzadehab@tbzmed.ac.ir

[1] Department of Medical Nanotechnology, Faculty of Advanced Medical Sciences, Tabriz University of Medical Sciences, Tabriz, Iran

[2] Department of Tissue Engineering, Faculty of Advanced Medical Sciences, Tabriz University of Medical Sciences, Tabriz, Iran

[3] Health Research Center, Chamran Hospital, Tehran, Iran

[4] Department of Chemistry, Farhangian University, Tehran, Iran

synthetic bioactive materials, have been considered for fabricating scaffolds [11]. They are mostly used in biomedical and pharmaceutical applications because of their favorable characteristics, such as high oxygen permeability, biocompatibility, biodegradability, and mechanical properties comparable to natural tissues [12]. PU-based nanofibers are suitable for skin tissue engineering and wound dressing fields as PU offers advantages, including excellent mechanical properties, promoting epithelization, and porous structure for nutrient and gas exchanges [13–15]. In addition, the barrier properties of PU-based nanofibers do not allow bacteria to reach the internal surface of the wound [16]. Functional PUs with desired properties such as biodegradability, blood compatibility, and self-assembly has also been investigated for biomedical applications [17]. In a recent study [18], it was reported that the incorporation of PCL to PU electrospun solution in the ratio of 1:2 could present good pore size, nanofiber diameter size, and mechanical properties. Therefore, the development of a composite nanofiber with PU and PCL using electrospinning technology can address the multi-aspects of scaffolds for tissue engineering. However, the low hydrophilicity of PU-based scaffolds is one of their drawbacks that limit their applications [19]. The surface modification of PU nanofibers with nanoparticles can overcome the hydrophobicity of scaffolds thanks to the presence of different polar groups in PU [20]. Among candidates to be used for skin tissue engineering, GNPs can be considered as attractive nanostructures because of their biocompatibility, low toxicity, and electrical conductivity properties for affecting the cell behaviors [21–23]. It has been reported that electrical conductivity is another factor that can influence cell attachment and proliferation properties [24]. In addition, the positive effects of GNPs on neovascularization and accelerating the wound healing process have been mentioned [25]. Yang et al. reported the fabrication of GNPs doped PCL/gelatin fibers for wound healing application. Their results showed effective antimicrobial activity, biocompatibility, and adequate wound healing property [26]. However, there are no sufficient studies on using GNPs for skin tissue engineering.

In the past years, studies have been conducted on the fabricating scaffolds containing natural oils. Soybean is a natural material composed of proteins, carbohydrates, oil fractions, and isoflavones [27, 28]. The oil fraction of soybean include polyunsaturated oils (linoleic acid (51%), oleic acid (25%), palmitic acid (11%), linolenic acid (9%), and stearic acid (4%) residues) [29, 30]. SO possesses various properties that attract pharmaceutical, cosmetics, and food industries for the delivery of bioactive molecules [31]. SO with essential fatty acids can present antioxidant, anti-inflammatory, and epithelizing properties. Soybean-modified polyamide-6 mats were found to support a higher percentage of fibroblast attachment by visible contact points with the surrounding fibers and ECM release of cells, well-spread and elongated morphology, and migration [32]. Moreover, the promotion of cell adhesion and proliferation by SO-based PU networks has been reported [33]. The epoxidized form of SO has been applied for the cross-linking of α-cellulose-based scaffolds with high porosity and biocompatibility [34].

The present study aimed to develop biocompatible and cell responsive electrospun PU/PCL nanofiber scaffolds containing SO and GNPs for tissue engineering applications. For this purpose, the fabricated scaffolds were subjected to physicochemical characterization such as chemical composition, morphology, surface roughness, mechanical properties, wettability, and electroconductivity. The biocompatibility evaluations of the fabricated nanofibers were conducted by proliferation and attachment of the NIH-3T3 fibroblast cell line.

2 Materials and Methods

2.1 Materials

PU, PCL, $HAuCl_4$, tri-sodium citrate, and (3-[4, 5-dimethylthiazol-2-yl]-2, 5-diphenyltetrazolium bromide (MTT) were supplied from Sigma-Aldrich. Tetrahydrofuran (THF), N, N Dimethylformamide (DMF), and Dimethyl Sulfoxide (DMSO) were purchased from Merck. Roswell Park Memorial Institute medium (RPMI) 1640 medium, Fetal Bovine Serum (FBS), Trypsin–EDTA, and Penicillin–Streptomycin (Pen-Strep) were obtained from GIBCO.

2.2 Methods

2.2.1 Synthesis of GNPs

GNPs were synthesized based on the reduction of Au ions by tri-sodium citrate. To synthesize the GNPs, the aqueous solution of $HAuCl_4$ (1 mM, 20 ml) was stirred under 100–150 ℃ to reach the boiling point. Then, tri-sodium citrate solution (1% w/v, 2 ml) was quickly added to the boiling $HAuCl_4$ solution. After the color changed from light yellow to dark red, the reaction was stopped, and the obtained GNPs were cooled at room temperature.

2.2.2 Preparation of Different Nanofibrous Mats by Electrospinning

PU/PCL nanofibers were prepared with regards to the previous research [18] with some modifications. For preparation of the electrospinning solution, 0.189 g PU and 0.094 g PCL were dissolved in DMF and THF (4:1). The mixture was

stirred for 18 h to get a homogeneous solution. To fabricate the SO-loaded nanofibers (PU/PCL/SO), initially, the PU/PCL solution was prepared similarly to the above section, and then SO with a concentration of 30% v/v was added to it. For preparation of the electrospun solution of PU/PCL/SO/GNP composite nanofibers, after obtaining PU/PCL solution, the centrifuged GNPs (2 ml) and SO (30% v/v) were added to it, respectively. The same electrospinning conditions were applied to all the samples. For electrospinning, 3 ml of the solution was placed in a syringe and fitted into the device. The solution was injected at the rate of 2 ml/h, and the collector distance from the needle tip was adjusted to 15 cm. To charge the solution, a 20 kV voltage was applied. The formed electrospun nanofibers were collected over the aluminum foil placed on the collector and dried in a vacuum for 24 h.

2.2.3 Physicochemical Characterization of Nanofibrous Mats

ATR-FTIR (Bruker) was used to indicate the surface chemical structure of the electrospun nanofibrous mats. In addition, this analysis was used to determine whether SO was successfully integrated into PU/PCL scaffolds. The spectrum was recorded within the range of 600–4000 cm^{-1}.

The morphology and diameter size distribution of prepared nanofibers was investigated using SEM (MIRA3, Tescan). For this purpose, the gold sputter-coated samples were imaged by SEM. The nanofiber diameter size distribution was determined by ImageJ software.

To evaluate the hydrophilicity of the fabricated nanofibers, the water contact angle measurements were determined by a contact angle instrument (Dataphysics, OCA 15 plus). To this, the nanofibers were cut into square shapes (1×1 cm), and water droplets (4 µl) were gently placed on the nanofiber's surfaces. The images were recorded by CCD camera and the contact angles were calculated by the image analysis software.

To assessment the surface roughness of the fabricated nanofibers, AFM (Nanosurf, Nanosurf Mobile- S) was used. The topographic and phase images were obtained.

For the electrical conductivity assessment of the fabricated nanofibers, the standard four-probe technique was used [35] by measuring the voltage in different currents. Finally, the resistance was calculated. The electrical conductivity of the nanofibers can be calculated by inverting the resistance value of them.

2.2.4 Mechanical Characterization

To evaluate the mechanical properties of the fabricated nanofibers, the tensile strength was measured using a mechanical instrument (Instron Z010, Zwick/Roell). For this purpose, the rectangular-shaped (50 mm × 10 mm) samples were placed into the testing machine, and tests were conducted at a strain rate of 5 mm/min.

2.2.5 Biocompatibility of the Nanofibers

We used fibroblast cell line to investigate the biocompatibility studies due to the importance of these cells in the injured tissues [13]. NIH-3T3 fibroblast cell lines were cultured in RPMI 1640 medium complemented with 10% v/v FBS and 1% v/v Pen-Strep and incubated at 37 °C under 5% CO_2. All the nanofibers were punched into the small disk shapes and sterilized with UV light for 60 min. After reaching 70–80% confluency, the cells were detached with trypsin–EDTA and seeded on the surface of the scaffolds (5×10^3 cells/each well). The cell-seeded samples were incubated under standard culture conditions for several days. The biocompatibility of the fabricated nanofibers was evaluated by the MTT assay. At the predetermined times (3 and 5 days after seeding), the culture medium was replaced with MTT solution (3 mg/ml) and a new medium containing FBS. After incubation for 4 h at 37 °C, the supernatant was discarded and replaced with 150 µl DMSO to dissolve the formazan crystals. Finally, the absorbance of the samples was measured by a Microplate Reader (Awareness Technology).

The cell attachment on the surface of nanofibers was studied to evaluate the compatibility of the fabricated mats for fibroblast attachment, connection, and migration. For this investigation, the NIH-3T3 fibroblast cells were placed on the surface of each nanofiber according to the previous section and incubated for three days. Then, the medium was removed, the cell-seeded scaffolds were rinsed with fresh phosphate-buffered saline (PBS), and cells were fixed with glutaraldehyde (4% v/ v in PBS) for 20 min. In the next step, ethanol solutions (50, 60, 70, 80, 90, and 100% v/v) were applied to dehydrate the samples. Finally, the attached cells on the nanofiber's surfaces were imaged by SEM.

2.3 Statistical Analysis

Statistical analysis was performed by one-way analysis of variance (ANOVA) via Graph PAD Prism software (version 8.0.2). All the experimental results were presented

as means ± standard deviations, and p value < 0.05 was determined as the statistical significance.

3 Results and Discussion

3.1 Physicochemical Characterization of Nanofibrous Mats

3.1.1 ATR-FTIR Spectroscopy

In this work, ATR-FTIR spectroscopy was used to indicate the chemical composition of the nanofiber's surfaces. Figure 1 displays the peaks of pristine SO, PU/PCL, PU/PCL/SO, and PU/PCL/SO/GNPs composite nanofibers. As shown in Fig. 1, the characteristic band of PCL was observed at 1725 cm^{-1} which was assigned to the stretching vibration of carbonyl groups (C=O). The peaks near 2868–2952 cm^{-1} were attributed to the C−H stretching vibration of PCL units. About PU, the characteristic absorption peak at 1531 cm^{-1} was corresponded to the amide groups of N−H and C−N. About SO, the bands around 2854–2924 cm^{-1} and 1462 cm^{-1} were attributed to the −CH3 and −CH2 stretching vibrations. In addition, peaks at 3010 (CH=CH), 1709 (−COOC−), and 1083 cm^{-1} (−C−O−C−) were observed, that could show the existence of unsaturated double bonds of SO [36]. From the spectra, it can be seen that the peak of hydrocarbon bonds (methyl stretching), which is seen around 2900 cm^{-1}, has increased in SO and samples mixed with it. Since soy is a fatty acid, its integration into the PU/PCL mesh increases the elongation of methyl, which can be seen in the spectra of SO, PU/PCL/SO, and PU/PCL/SO/GNP. Therefore, SO forms chain entanglements instead of covalently binding to PU/PCL mass materials. This increase in methyl elongation and methyl groups indicates that SO has been successfully integrated into the samples.

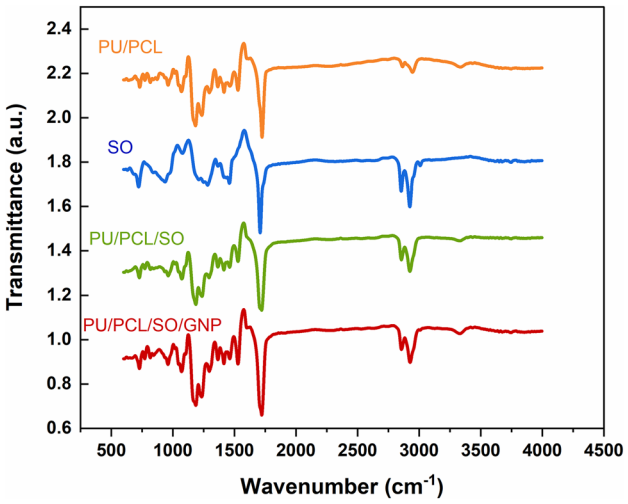

Fig. 1 FTIR spectra of pristine SO, PU/PCL, PU/PCL/SO, and PU/PCL/SO/GNPs composite nanofibers

3.1.2 Morphological Characterization of Nanofibrous Mats

In tissue engineering and fabrication of appropriate fibers for biomedical applications, the study of their morphology is very important in terms of fiber diameter [37, 38]. Fiber diameter is an important parameter for cellular signaling that can ultimately significantly affect cell differentiation and function. Optimizing fiber diameters is critical to achieving a well function and biocompatible scaffold [39, 40]. In this work, the fabricated PU/PCL, PU/PCL/SO, and PU/PCL/SO/GNP composite nanofibers were morphologically investigated through SEM images. Figure 2 shows the different groups of nanofibers prepared in this study. The fibers showed suitable morphology and free of beads characteristics. The presence of a porous network was also observed despite the distinct fibers. In addition, based on the SEM images, it was observed that the presence of SO in the nanofiber structure has increased the diameter of the nanofibers and their fusion. It also appears that the fibrous structure has lost its homogeneous shape. But on the other hand, it was observed that the presence of GNPs in the PU/PCL/SO/GNP fibers has created a homogeneous and uniform fiber structure. Generally, the combination of SEM micrographs and ImageJ analysis of the nanofiber samples shows that the presence of SO and GNPs increases the diameter of the fibers. This phenomenon is thought to be due to the being ejected of more solutes at the tip of the Taylor cone, which increases the fiber diameter. This has been observed in previous studies [41, 42]. These results demonstrated the successful incorporation of SO into PU/PCL mesh materials as well as the successful incorporation of GNPs.

3.1.3 Surface Water Absorption of Nanofibrous Mats

Surface hydrophilicity is one of the important parameters that affect the biological properties of fibers and provide improved properties in terms of cell growth and proliferation [43, 44]. For this purpose, in the present study, to evaluate the mentioned feature, measuring the contact angle of the water droplet was used. The contact angle assessment is based on the theta angle, and the lower theta angle lead to the more hydrophilicity of the surface. In addition, according to the previous studies, a contact angle close to at least 90 indicates a hydrophobic surface [41]. In the present study, the contact angle of the PU/PCL fibers is more than 113 degrees, which means incomplete wetting. On the other hand, contact angle measurements for the PU/PCL/SO and PU/PCL/SO/GNP fibers show 91 and 76 degrees, respectively, indicating good wetting of these scaffolds. In this part

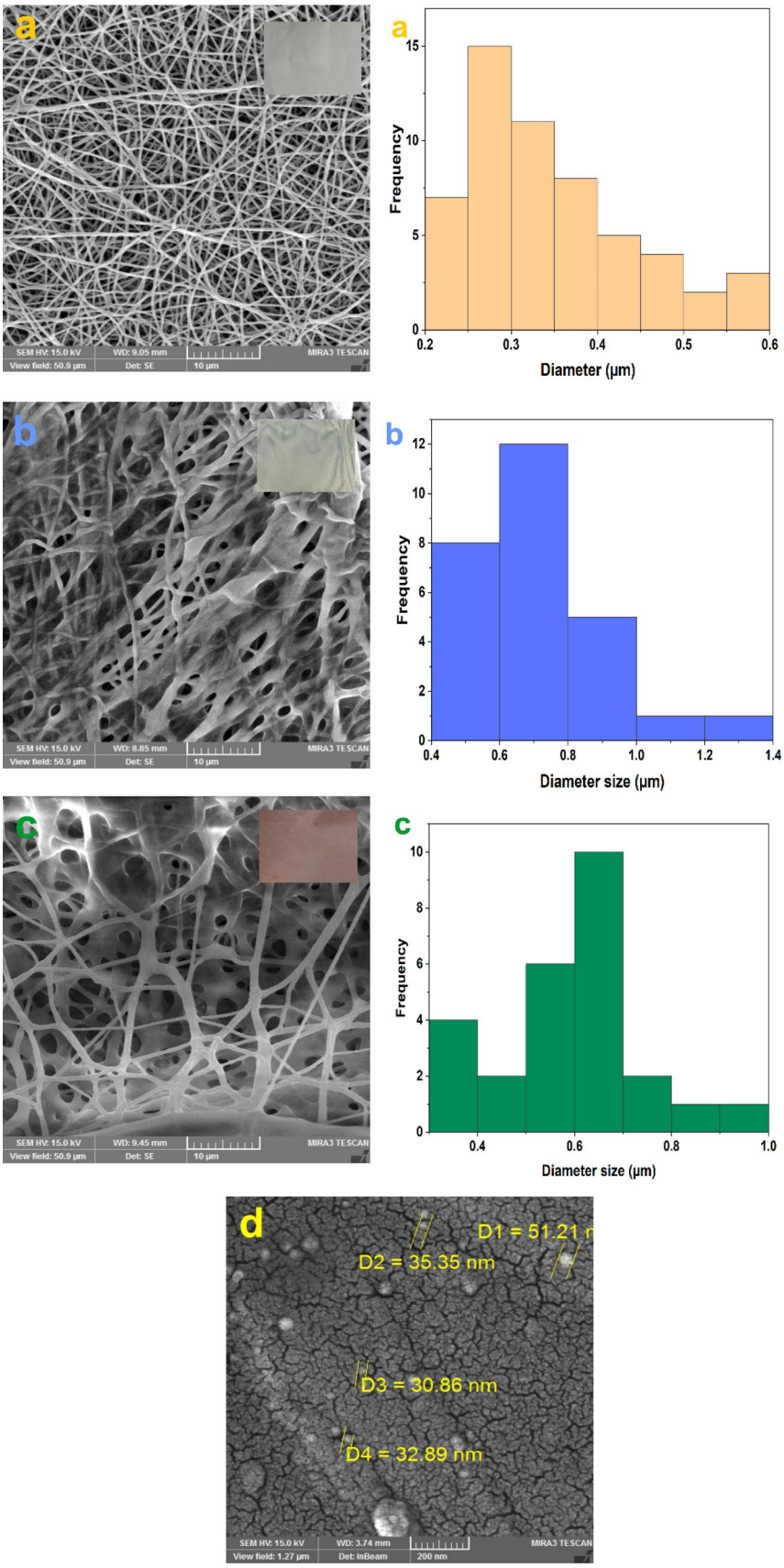

Fig. 2 SEM images and size distribution of **a** PU/PCL nanofibers, **b** PU/PCL/SO nanofibers, **c** PU/PCL/SO/GNP nanocomposite fibers, and **d** GNPs

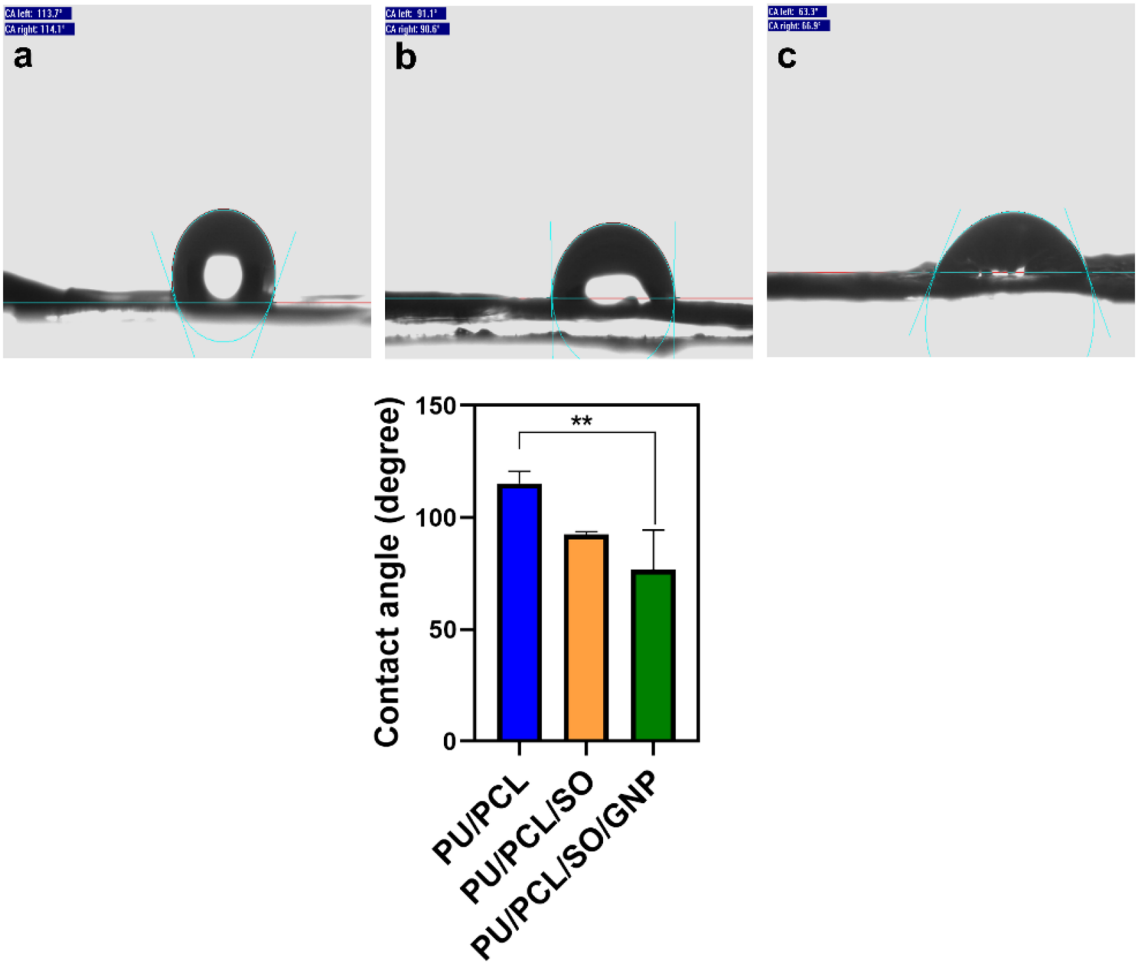

Fig. 3 Contact angle images and measurements of **a** PU/PCL nanofibers, **b** PU/PCL/SO nanofibers, and **c** PU/PCL/SO/GNP nanocomposite fibers ***$p < 0.001$

of the study, several measurements were performed on the samples at different spatial locations. As shown in Fig. 3, the fibers containing SO have more hydrophilic surface properties than oil-free fiber (PU/PCL fiber). In addition, as it was reported in previous studies that the use of GNPs decreases the contact angle [23, 45], in this study, it was also observed that the presence of GNP leads to a further decrease in the water contact angle and thus more wettability. This is most likely because the contact angle of GNPs is about $82.3° \pm 8.0°$, as reported by Lucio et al. [46]. Accordingly, the decrease in water contact angle can be related to the more hydrophilic nature of GNPs than PU/PCL. Finally, it was demonstrated that the presence of GNPs led to more wettability of the PU/PCL/SO/GNP nanofibers compared to the other samples. It was demonstrated that the presence of GNPs along with SO in the structure of PU/PCL/SO/GNP fibers caused a significant increase ($p < 0.01$) compared to the PU/PCL nanofiber in terms of surface hydrophilicity.

3.1.4 The Surface Roughness Study

To increase the biocompatibility of tissue engineering scaffolds, achieving higher hydrophilicity with surface roughness is critical, because it can create a favorable environment for the appropriate function of cells and their proliferation [47]. As shown in Fig. 4a, PU/PCL nanofibers show a surface with noticeable roughness. The rough surface of PU/PCL nanofibers was altered by the incorporation of SO (Fig. 4b). It has also been observed that the surface roughness of the sample encoded with PU/PCL/SO/GNP (Fig. 4c) is more balanced compared to the pure PU/PCL nanofibers or PU/PCL nanofibers loaded with SO. Therefore, it was proved that the great change in the surface is attributed to the presence of GNPs, which causes a significant surface smoothness. Meanwhile, SO does not have a considerable effect on the surface nature of PU/PCL nanofibers, and only their presence, along

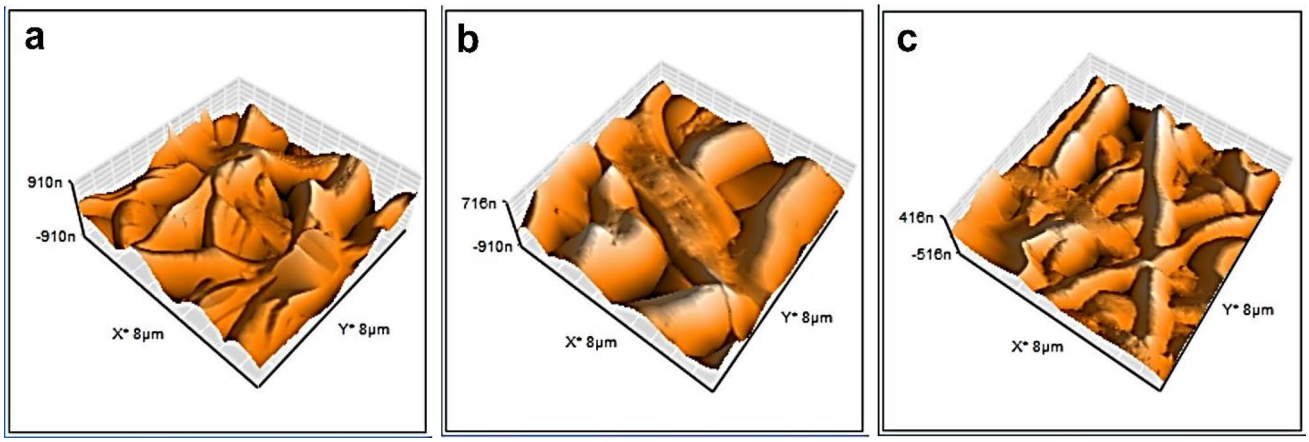

Fig. 4 AFM results of **a** PU/PCL nanofibers, **b** PU/PCL/SO nanofibers, and **c** PU/PCL/SO/GNP nanocomposite fibers

Table 1 Electrical conductivity measurement of the nanofibers

Sample	Volume conductivity (S/cm)
PU/PCL	1.06E-10
PU/PCL/SO	2.82E-10
PU/PCL/SO/GNP	3.32E-10

with GNPs, causes a more balanced surface roughness, which is essential for better interaction with cells.

3.1.5 Electrical Conductivity Measurement of the Nanofibers

The distribution of GNPs throughout the scaffold is an effective strategy to increase electrical conductivity [48]. GNPs, known as biocompatible nanostructures, have great potential for enhancing intercellular electrical communication. Various studies have shown that the presence of GNPs in various structures made of materials such as alginate, collagen, and poly (2-hydroxyethyl methacrylate) increases the electrical conductivity of the scaffold and better function of cardiomyocytes and effective differentiation of mesenchymal cells [49–51]. In this study, the electrical conductivity of PU/PCL, PU/PCL/SO, and PU/PCL/SO/GNP nanofibers was reported according to Table 1. It was observed that both oil and GNPs caused a significant increase in electrical conductivity and acted well as electrical stimuli.

3.2 Mechanical Characterization of the Nanofibers

Mechanical properties strongly depend on the composition of the structure. To estimate the effect of GNP and SO on tensile properties, the stress–strain curves for various samples were plotted (Fig. 5). In addition, Table 2 reports the mechanical properties of the samples. It has been observed that the mechanical properties showed a lower value for PU/PCL/SO mesh compared to pure PU/PCL nanofibers. The

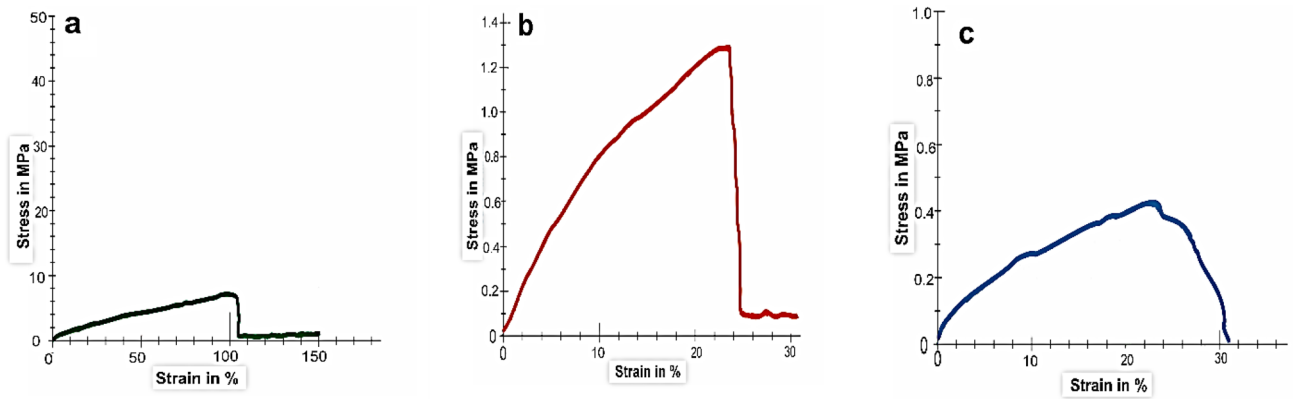

Fig. 5 Stress–strain curve of electrospun **a** PU/PCL nanofibers, **b** PU/PCL/SO nanofibers, and **c** PU/PCL/SO/GNP nanocomposite fibers

Table 2 Mechanical properties of the prepared nanofibers

Sample	Tensile strength (MPa) Young's modulus (MPa)
PU/PCL	8.29 ± 1.20 25.23 ± 1.75
PU/PCL/SO	0.95 ± 0.29 11.04 ± 4.34
PU/PCL/SO/GNP	0.38 ± 0.052 8.12 ± 4.26

results showed that the combination of SO leads to statistically significant data. This reduction is due to the greater flexibility that is more appropriate for some tissue engineering applications [52]. Various surface factors, such as porosity and fiber distribution, can be effective in the mechanical properties. A compound that increases porosity reduces the tensile strength of the nanofibers, although the excellent alignment of the nanofibers increases the strength and thus creates more elasticity.

3.3 Biocompatibility of the Nanofibers

3.3.1 MTT Assay

It is expected that antimicrobial substances such as GNPs should always be highly biocompatible when used in clinical applications and not be toxic to normal cells [53, 54]. Thus, to investigate the biocompatibility of the fabricated nanofibers, MTT assay was performed on days 3 and 5. On the third day, all the samples showed a significant enhancement in optical density (OD) compared to the control sample (Fig. 6). As can be seen, because of the excellent biocompatibility, the fabricated PU/PCL showed high cell viability. On the other hand, the PU/PCL mixture with SO did not change cell viability. This can be due to the SO's biocompatibility with human cells. In addition, it was observed, when PU/PCL mixed with GNP (PU/PCL/SO/GNP), the cell viability slightly decreased, but it remained within acceptable limits. In addition, there is no significant difference between the study groups on the third and fifth days. These confirm that the presence of GNP and SO in the structure of nanofibers has not led to a negative effect on their biocompatibility. Our research, as well as that of others [41, 55, 56], has shown that cell proliferation increase in GNP-bound substances.

3.3.2 Cell Attachment Study

Various surface properties, including different chemical groups, hydrophilicity, and roughness, can affect cell adhesion and alter cell viability [57, 58]. As various studies have shown an increase in cell binding following an increase in hydrophilicity [59, 60], our results have also demonstrated that the addition of SO and GNP increases hydrophilicity and ultimately increases cell adhesion and viability. As mentioned earlier, incorporating SO and GNP has resulted in a rougher surface, followed by increased cell attachment. This can be seen in Fig. 7.

4 Conclusion

In the present study, the electrospun PU/PCL, PU/PCL/SO, and PU/PCL/SO/GNP nanofibers were fabricated and characterized. The presence of GNPs in the PU/PCL/SO/GNP fibers has created a homogeneous and uniform fiber structure. In addition, the AFM results indicated a significant surface smoothness for PU/PCL/SO/GNP nanocomposite mats. The wettability behavior of the nanofibers was measured, and PU/PCL/SO/GNP nanocomposite fibers showed more hydrophilicity compared to the other groups. The reinforcement of PU/PCL nanofibers with SO and GNP leads to an increase in electroconductivity. The cytocompatibility studies demonstrated the fabricated scaffolds, especially PU/PCL/SO/GNP nanocomposite fibers, have great potential to be applied as biocompatible biomaterials to support cellular adhesion and tissue engineering.

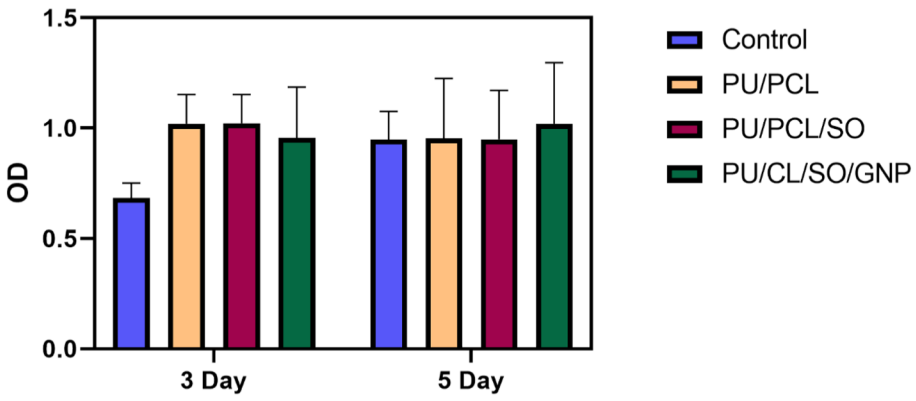

Fig. 6 The MTT results of PU/PCL, PU/PCL/SO, and PU/PCL/SO/GNP nanocomposite fibers at 3 and 5 days after seeding

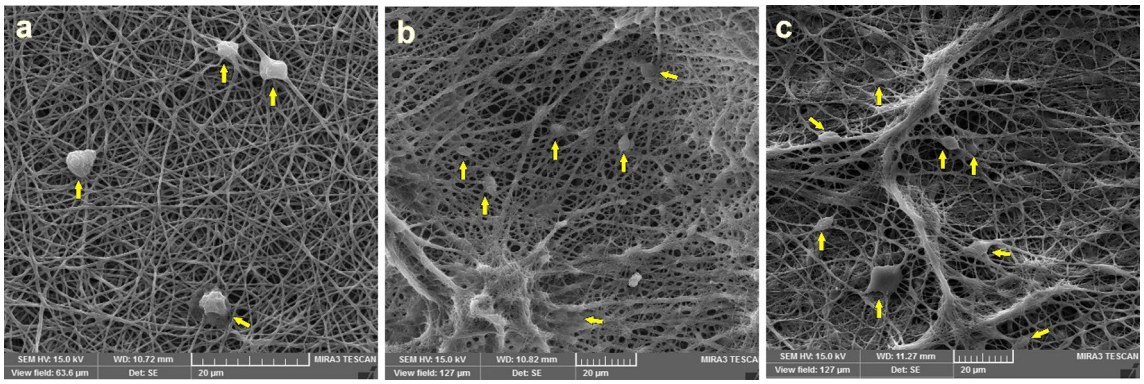

Fig. 7 SEM images shows the NIH-3T3 fibroblast cells attachment on the **a** PU/PCL, **b** PU/PCL/SO, and **c** PU/PCL/SO/GNP nanocomposite fibers at 3rd day after seeding

Supplementary Information The online version contains supplementary material available at https://doi.org/10.1007/s42235-023-00345-x.

Acknowledgements The authors would like to thank the Department of Medical Nanotechnology, Faculty of Advanced Medical Sciences, Tabriz University of Medical Sciences for financial supporting this project (Grant NO: 62379).

Author Contributions NA: conceptualization, methodology, investigation, formal analysis, and writing—review and editing. ARDB: writing—original draft and writing—review and editing. HS and SK: methodology and investigation. ANA and AA: project administration, conceptualization, supervision, resources, and funding acquisition.

Funding This study was funded by Department of Medical Nanotechnology, Faculty of Advanced Medical Sciences, Tabriz University of Medical Sciences (Grant NO: 62379).

Data Availability Not applicable.

Declarations

Conflict of Interest The authors declare that they have no conflict of interest.

Ethical Approval The ethical approval for this paper was obtained from research ethics committee of Tabriz University of Medical Sciences (IR.TBZMED.VCR.REC.1397.487).

References

1. Jadbabaei, S., Kolahdoozan, M., Naeimi, F., & Ebadi-Dehaghani, H. (2021). Preparation and characterization of sodium alginate–PVA polymeric scaffolds by electrospinning method for skin tissue engineering applications. *RSC Advances, 11*(49), 30674–30688. https://doi.org/10.1039/D1RA04176B
2. Madni, A., Kousar, R., Naeem, N., & Wahid, F. (2021). Recent advancements in applications of chitosan-based biomaterials for skin tissue engineering. *J Biores and Bioprod, 6*(1), 11–25. https://doi.org/10.1016/j.jobab.2021.01.002
3. Li, Y., Li, X., Zhao, R., Wang, C. I., Qiu, F. P., Sun, B., Ji, H., Qui, J., & Wang, C. (2017). Enhanced adhesion and proliferation of human umbilical vein endothelial cells on conductive PANI-PCL fiber scaffold by electrical stimulation. *Materials Science and Engineering, 72*, 106–112. https://doi.org/10.1016/j.msec.2016.11.052
4. Yao, R. J., Wang, Y., Zhang, B., Liu, J., Zhang, N. H., He, J., Meng, G. L., Jiang, B., Wang, Sh. L., & Wu, F. (2021). Critical role of silicon in directing the bio-inspired mineralization of gelatin in the presence of hydroxyapatite. *Journal of Bionic Engineering, 18*(6), 1413–1429. https://doi.org/10.1007/s42235-021-00084-x
5. Keirouz, A., Chung, M. C., Kwon, J. H., Fortunato, G., & Radacsi, N. (2020). 2D and 3D electrospinning technologies for the fabrication of nanofibrous scaffolds for skin tissue engineering: A review. *Wiley Interdiscipl Review, 12*(4), e1626.
6. Dehghan-Manshadi, N., Fattahi, S., Hadizadeh, M., Nikukar, H., Moshtaghioun, S. M., & Aflatoonian, B. (2019). The influence of elastomeric polyurethane type and ratio on the physicochemical properties of electrospun polyurethane/silk fibroin hybrid nanofibers as potential scaffolds for soft and hard tissue engineering. *Euro Poly J, 121*, 109294.
7. Chen, SXu., Liu, B., Carlson, M. A., Gombart, A. F., Reilly, D. A., & Xie, J. W. (2017). Recent advances in electrospun nanofibers for wound healing. *Nanomedicine, 12*(11), 1335–1352.
8. Olczyk, P., Mencner, Ł, & Komosinska-Vassev, K. (2014). The role of the extracellular matrix components in cutaneous wound healing. *BioMed Res Inter*. https://doi.org/10.1155/2014/747584
9. Ma, Z. I., Xu, Y. H., Jiang, Y. G., Hu, X. H., & Zhang, D. U. (2020). BTO/P (VDF-TrFE) nanofiber-based artificial lateral line sensor with drag enhancement structures. *Journal of Bionic Engineering, 17*(1), 64–75. https://doi.org/10.1007/s42235-020-0005-8
10. Zhang, Y. H., Li, T. S., Zhang, S. H., Jiang, L., Xia, J. Y., Xie, J., Chen, K., Bao, L., Lei, J. X., & Wang, J. (2022). Room-temperature, energy storage textile with multicore-sheath structure obtained via in-situ coaxial electrospinning. *Chemical Engineering Journal, 436*, 135226.
11. Joseph, J., Patel, R. M., Wenham, A., & Smith, J. R. (2018). Biomedical applications of polyurethane materials and coatings. *Trans of the IMF, 96*(3), 121–129. https://doi.org/10.1080/00202967.2018.1450209
12. Naureen, B., Haseeb, A. S. M. A., Basirun, W. J., & Muhamad, F. (2021). Recent advances in tissue engineering scaffolds based on polyurethane and modified polyurethane. *Materials Science and Engineering, 118*, 111228.
13. Sofi, H. S., Akram, T., Tamboli, A. H., Majeed, A., Shabir, N., & Sheikh, F. A. (2019). Novel lavender oil and silver nanoparticles

simultaneously loaded onto polyurethane nanofibers for wound-healing applications. *Inter J Pharm., 569*, 118590.
14. Sahraro, M., Yeganeh, H., & Sorayya, M. (2016). Guanidine hydrochloride embedded polyurethanes as antimicrobial and absorptive wound dressing membranes with promising cytocompatibility. *Materials Science and Engineering, 59*, 1025–1037. https://doi.org/10.1016/j.msec.2015.11.038
15. Liu, X. G., Niu, Y. I., Chen, K. C., & Chen, S. G. (2017). Rapid hemostatic and mild polyurethane-urea foam wound dressing for promoting wound healing. *Mat Sci Eng, 71*, 289–297. https://doi.org/10.1016/j.msec.2016.10.019
16. Abrigo, M., McArthur, S. L., & Kingshott, P. (2014). Electrospun nanofibers as dressings for chronic wound care: advances, challenges, and future prospects. *Macromolecular Bioscience, 14*(6), 772–792. https://doi.org/10.1002/mabi.201300561
17. Bao, L., Luo, X., Zhang, D., Lei, J. X., Cao, Q., & Wang, J. (2014). Synthesis, characterization, and self-assembly behaviors of a biodegradable and anti-clotting poly (EDTA-diol-co-butylene adipate glycol urethanes). *Journal of Materials Chemistry, 2*(35), 5862–5871. https://doi.org/10.1039/C4TB00603H
18. Karkan, S. F., Rahbarghazi, R., Davaran, S., Kaleybar, L. S., Khoshfetrat, A. B., Heidarzadeh, M., Zolali, E., & Akbarzadeh, A. (2021). Electrospun polyurethane/poly (ε-caprolactone) nanofibers promoted the attachment and growth of human endothelial cells in static and dynamic culture conditions. *Microvas Res, 133*, 104073.
19. Bužarovska, A., Dinescu, S., Lazar, A. D., Serban, M., Pircalabioru, G. G., Costache, M., Gualandi, C., & Avérous, L. (2019). Nanocomposite foams based on flexible biobased thermoplastic polyurethane and ZnO nanoparticles as potential wound dressing materials. *Materials Science and Engineering, 104*, 109893.
20. Shahrousvand, M., Hoseinian, M. S., Ghollasi, M., Karbalaeimahdi, A., Salimi, A., & Tabar, F. A. (2017). Flexible magnetic polyurethane/Fe2O3 nanoparticles as organic-inorganic nanocomposites for biomedical applications: properties and cell behavior. *Materials Science and Engineering, 74*, 556–567. https://doi.org/10.1016/j.msec.2016.12.117
21. Pourjavadi, A., Doroudian, M., Ahadpour, A., & Azari, S. (2019). Injectable chitosan/κ-carrageenan hydrogel designed with au nanoparticles: A conductive scaffold for tissue engineering demands. *Inter J Biol Macromol, 126*, 310–317. https://doi.org/10.1016/j.ijbiomac.2018.11.256
22. Pajerski, W., Ochonska, D., Brzychczy-Wloch, M., Indyka, P., Jarosz, M., Golda-Cepa, M., Sojka, Z., & Kotarba, A. (2019). Attachment efficiency of gold nanoparticles by Gram-positive and Gram-negative bacterial strains governed by surface charges. *J Nanoparticle Res, 21*, 186. https://doi.org/10.1007/s11051-019-4617-z
23. Joseph, B., Ninan, N., Visalakshan, R. M., Denoual, C., Bright, R., Kalarikkal, N., Grohens, Y., Vasilev, K., & Thomas, S. (2021). Insights into the biomechanical properties of plasma treated 3D printed PCL scaffolds decorated with gold nanoparticles. *Composit Sci Technol., 202*, 108544.
24. Zarei, M., Samimi, A., Khorram, M., Abdi, M. M., & Golestaneh, S. I. (2021). Fabrication and characterization of conductive polypyrrole/chitosan/collagen electrospun nanofiber scaffold for tissue engineering application. *Inter J Biol Macromol, 168*, 175–186. https://doi.org/10.1016/j.ijbiomac.2020.12.031
25. Radwan-Pragłowska, J., Janus, Ł, Piątkowski, M., Bogdał, D., & Matýsek, D. (2020). Hybrid bilayer PLA/chitosan nanofibrous scaffolds doped with ZnO, Fe3O4, and Au nanoparticles with bioactive properties for skin tissue engineering. *Polymers, 12*(1), 159. https://doi.org/10.3390/polym12010159
26. Yang, X. L., Yang, J. C., Wang, L., Ran, B., Jia, Y. X., Zhang, L. M., Yang, G., Shao, H. W., & Jiang, X. G. (2017). Pharmaceutical intermediate-modified gold nanoparticles: against multidrug-resistant bacteria and wound-healing application via an electrospun scaffold. *ACS Nano, 11*(6), 5737–5745. https://doi.org/10.1021/acsnano.7b01240
27. Perut, F., Montufar, E. B., Ciapetti, G., Santin, M., Salvage, J., Traykova, T., Planell, J. A., Ginebra, M. P., & Baldini, N. (2011). Novel soybean/gelatine-based bioactive and injectable hydroxyapatite foam: Material properties and cell response. *Acta Biomaterialia, 7*(4), 1780–1787. https://doi.org/10.1016/j.actbio.2010.12.012
28. Grieshop, C. M., & Fahey, G. C. (2001). Comparison of quality characteristics of soybeans from Brazil, China, and the United States. *J Agri Food Chem, 49*(5), 2669–2673. https://doi.org/10.1021/jf0014009
29. Tığlı Aydın, R. S., Hazer, B., Acar, M., & Gümüşderelioğlu, M. (2013). Osteogenic activities of polymeric soybean oil-g-polystyrene membranes. *Polymer Bulletin, 70*, 2065–2082. https://doi.org/10.1007/s00289-013-0976-2
30. Ilter, S., Hazer, B., Borcakli, M., & Atici, O. (2001). Graft copolymerisation of methyl methacrylate onto a bacterial polyester containing unsaturated side chains. *Macro Chem Phy, 202*(11), 2281–2286.
31. Dhal, S., Pal, K., & Giri, S. (2020). Transdermal delivery of gold nanoparticles by a soybean oil-based oleogel under iontophoresis. *ACS Applied Bio Mater, 3*(10), 7029–7039. https://doi.org/10.1021/acsabm.0c00893
32. Dias, F. T. G., Ingracio, A. R., Nicoletti, N. F., Menezes, F. C., Agnol, L. D., Marinowic, D. R., Soares, R. M. D., Costa, J. C., & d., Falavigna, A., & Bianchi, O. (2019). Soybean-modified polyamide-6 mats as a long-term cutaneous wound covering. *Materials Science and Engineering, 99*, 957–968. https://doi.org/10.1016/j.msec.2019.02.019
33. Miao, S., Sun, L. I., Wang, P., Liu, R., Su, Z. G., & Zhang, S. P. (2012). Soybean oil-based polyurethane networks as candidate biomaterials: Synthesis and biocompatibility. *Euro J Lipid Sci Technol, 114*(10), 1165–1174.
34. Pour-Esmaeil, S., Sharifi-Sanjani, N., Khoee, S., & Taheri-Qazvini, N. (2020). Biocompatible chemical network of α-cellulose-ESBO (epoxidized soybean oil) scaffold for tissue engineering application. *Carbohy Poly, 241*, 116322.
35. Afjeh-Dana, E., Naserzadeh, P., Nazari, H., Mottaghitalab, F., Shabani, R., Aminii, N., Mehravi, B., Tajik Rostami, F., Joghataei, M. T., Mousavizadeh, K., & Ashtari, K. (2019). Gold nanorods reinforced silk fibroin nanocomposite for peripheral nerve tissue engineering applications. *Inter J Biol Macromol, 129*, 1034–1039. https://doi.org/10.1016/j.ijbiomac.2019.02.050
36. Bao, L., Bian, L. C., Zhao, M., Lei, J. X., & Wang, J. (2014). Synthesis and self-assembly behavior of a biodegradable and sustainable soybean oil-based copolymer nanomicelle. *Nano Res Lett, 9*, 391. https://doi.org/10.1186/1556-276X-9-391
37. Jenkins, T. L., & Little, D. (2019). Synthetic scaffolds for musculoskeletal tissue engineering: cellular responses to fiber parameters. *NPJ Regenerat Med, 4*, 15. https://doi.org/10.1038/s41536-019-0076-5
38. Saghati, S., Akbarzadeh, A., Del Bakhshayesh, A. R., Sheervalilou, R., & Mostafavi, E. (2018). *Electrospinning and 3D printing: prospects for market opportunity*. (Chapter 6: Electrospinning: From Basic Research to Commercialization). The Royal Society of Chemistry
39. Hsia, H. C., Nair, M. R., Mintz, R. C., & Corbett, S. A. (2011). The fiber diameter of synthetic bioresorbable extracellular matrix influences human fibroblast morphology and fibronectin matrix assembly. *Plas Reconstruct Surg, 127*(6), 2312–2320. https://doi.org/10.1097/prs.0b013e3182139fa4
40. Xu, J. Z., Fang, Q., Liu, Y. L., Zhou, Y., Ye, Z. Y., & Tan, W. S. (2021). In situ ornamenting poly (ε-caprolactone) electrospun fibers with different fiber diameters using chondrocyte-derived

extracellular matrix for chondrogenesis of mesenchymal stem cells. *Coll Surf Biointer., 197*, 111374.
41. Matson, T., Gootee, J., Snider, C., Brockman, J., Grant, D., & Grant, S. A. (2019). Electrospun PCL, gold nanoparticles, and soy lecithin composite material for tissue engineering applications. *Journal of Biomaterials Applications, 33*(7), 979–988. https://doi.org/10.1177/0885328218815807
42. Li, Z. Y., & Wang, C. (2013). *One-dimensional nanostructures: electrospinning technique and unique nanofibers* (pp. 15–29). Berlin Heidelberg: Springer.
43. Birhanu, G., Akbari Javar, H., Seyedjafari, E., Zandi-Karimi, A., & Dusti Telgerd, M. (2018). An improved surface for enhanced stem cell proliferation and osteogenic differentiation using electrospun composite PLLA/P123 scaffold. *Artificial Cells Nanomed Biotechnol, 46*(6), 1274–1281. https://doi.org/10.1080/21691401.2017.1367928
44. Del Bakhshayesh, A. R., Babaie, S., Niknafs, B., Abedelahi, A., Mehdipour, A., & Ghahremani-Nasab, M. (2022). High efficiency biomimetic electrospun fibers for use in regenerative medicine and drug delivery: A review. *Materials Chemistry and Physics*. https://doi.org/10.1016/j.matchemphys.2022.125785
45. Samadian, H., Khastar, H., Ehterami, A., & Salehi, M. (2021). Bioengineered 3D nanocomposite based on gold nanoparticles and gelatin nanofibers for bone regeneration: In vitro and in vivo study. *Scient Report, 11*, 13877. https://doi.org/10.1038/s41598-021-93367-6
46. Isa, L., Lucas, F., Wepf, R., & Reimhult, E. (2011). Measuring single-nanoparticle wetting properties by freeze-fracture shadow-casting cryo-scanning electron microscopy. *Nature Commun, 2*, 438. https://doi.org/10.1038/ncomms1441
47. Janvikul, W., Uppanan, P., Thavornyutikarn, B., Kosorn, W., & Kaewkong, P. (2013). Effects of surface topography, hydrophilicity and chemistry of surface-treated PCL scaffolds on chondrocyte infiltration and ECM production. *Procedia Eng, 59*, 158–165. https://doi.org/10.1016/j.proeng.2013.05.106
48. Baei, P., Jalili-Firoozinezhad, S., Rajabi-Zeleti, S., Tafazzoli-Shadpour, M., Baharvand, H., & Aghdami, N. (2016). Electrically conductive gold nanoparticle-chitosan thermosensitive hydrogels for cardiac tissue engineering. *Materials Science and Engineering, 63*, 131–141. https://doi.org/10.1016/j.msec.2016.02.056
49. Shevach, M., Maoz, B. M., Feiner, R., Shapira, A., & Dvir, T. (2013). Nanoengineering gold particle composite fibers for cardiac tissue engineering. *Journal of Materials Chemistry, 1*(39), 5210–5217. https://doi.org/10.1039/C3TB20584C
50. Orza, A., Soritau, O., Olenic, L., Diudea, M., Florea, A., Rus Ciuca, D., Mihu, C., Casciano, D., & Biris, A. S. (2011). Electrically conductive gold-coated collagen nanofibers for placental-derived mesenchymal stem cells enhanced differentiation and proliferation. *ACS Nano, 5*(6), 4490–4503. https://doi.org/10.1021/nn1035312
51. You, J. O., Rafat, M., Ye, G. J., & Auguste, D. T. (2011). Nanoengineering the heart: Conductive scaffolds enhance connexin 43 expression. *Nano letters, 11*(9), 3643–3648. https://doi.org/10.1021/nl201514a
52. Coverdale, B. D., Gough, J. E., Sampson, W. W., & Hoyland, J. A. (2017). Use of lecithin to control fiber morphology in electrospun poly (ε-caprolactone) scaffolds for improved tissue engineering applications. *J Biomed MaterRes, 105*(10), 2865–2874. https://doi.org/10.1002/jbm.a.36139
53. Shahi, S., Özcan, M., Maleki Dizaj, S., Sharifi, S., Al-Haj Husain, N., Eftekhari, A., & Ahmadian, E. (2019). A review on potential toxicity of dental material and screening their biocompatibility. *Toxicol Mech Meth, 29*(5), 368–377. https://doi.org/10.1080/15376516.2019.1566424
54. El-Naggar, M. E., Abd-Al-Aleem, A. H., Abu-Saied, M. A., & Youssef, A. M. (2021). Synthesis of environmentally benign antimicrobial dressing nanofibers based on polycaprolactone blended with gold nanoparticles and spearmint oil nanoemulsion. *J Mater Res Technol, 15*, 3447–3460. https://doi.org/10.1016/j.jmrt.2021.09.136
55. Deeken, C. R., Bachman, S. L., Ramshaw, B. J., & Grant, S. A. (2012). Characterization of bionanocomposite scaffolds comprised of mercaptoethylamine-functionalized gold nanoparticles crosslinked to acellular porcine tissue. *Journal of Materials Science, 23*, 537–546.
56. Chou, C. W., Hsu, S. H., & Wang, P. H. (2008). Biostability and biocompatibility of poly (ether) urethane containing gold or silver nanoparticles in a porcine model. *Journal of Biomedical Materials Research, 84*(3), 785–794. https://doi.org/10.1002/jbm.a.31387
57. Chang, H. I., & Wang, Y. (2011). *Cell responses to surface and architecture of tissue engineering scaffolds*. InTechOpen: In Regenerative medicine and tissue engineering-cells and biomaterials.
58. Banimohamad-Shotorbani, B., Rahmani Del Bakhshayesh, A., Mehdipour, A., Jarolmasjed, S., & Shafaei, H. (2021). The efficiency of PCL/HAp electrospun nanofibers in bone regeneration: A review. *Journal of Medical Engineering & Technology, 45*(7), 511–531. https://doi.org/10.1080/03091902.2021.1893396
59. Mishra, D., & Sinha, V. K. (2013). Polyurethane Foams from Cellulosic Waste and Natural Oil-based Polyols–a Modified Approach. *Poly from Rene Res, 4*(2), 85–107. https://doi.org/10.1177/204124791300400203
60. Tian, H. F., Guo, G. P., Fu, X. W., Yao, Y. Y., Yuan, L., & Xiang, A. (2018). Fabrication, properties and applications of soy-protein-based materials: A review. *Inter J Biol Macromol, 120*, 475–490. https://doi.org/10.1016/j.ijbiomac.2018.08.110